Available online at www.sciencedirect.com
SCIENCE DIRECT®
Molecular Phylogenetics and Evolution 38 (2006) 171–188
MOLECULAR PHYLOGENETICS AND EVOLUTION
www.elsevier.com/locate/ympev

Coalescent models reveal the relative roles of ancestral polymorphism, vicariance, and dispersal in shaping phylogeographical structure of an African montane forest robin

Rauri C.K. Bowie [a,*], Jon Fjeldså [b], Shannon J. Hackett [c], John M. Bates [c], Timothy M. Crowe [d]

[a] *DST/NRF Centre of Excellence in Birds at the FitzPatrick Institute, Department of Botany and Zoology, Stellenbosch University, Private Bag X1, Matieland 7602, South Africa*
[b] *Zoological Museum, University of Copenhagen, Universitietsparken 15, Copenhagen, Denmark*
[c] *Zoology Department, Field Museum of Natural History, 1400 South Lake Shore Drive, Chicago, IL 60605-2496, USA*
[d] *DST/NRF Centre of Excellence in Birds at the FitzPatrick Institute, Department of Zoology, University of Cape Town, Rondebosch 7701, South Africa*

Received 2 April 2005; revised 27 May 2005; accepted 1 June 2005
Available online 15 July 2005

Abstract

Although many studies have documented the effect of glaciation on the evolutionary history of Northern Hemisphere flora and fauna, this study is the first to investigate how the indirect aridification of Africa caused by global cooling in response to glacial cycles at higher latitudes has influenced the evolutionary history of an African montane bird. Mitochondrial DNA sequences from the NADH 3 gene were collected from 283 individual Starred Robins (*Pogonocichla stellata*, Muscicapoidea). At least two major vicariant events, one that separated the Albertine Rift from all but the Kenyan Highlands around 1.3–1.2 Myrs BP, and another that separated the Kenyan Highlands from the northern Eastern Arc, and the northern Eastern Arc from the south-central Eastern Arc between 0.9 and 0.8 Myrs BP appear to underlie much of the observed genetic diversity and structure within Starred Robin populations. These dates of divergence suggest a lack of recurrent gene flow; although the Albertine Rift and south-central Eastern Arc share haplotypes, based on coalescent analyses this can confidently be accounted for by ancestral polymorphism as opposed to recurrent gene flow. Taken collectively, strong evidence exists for recognition of four major ancestral populations: (1) Kenyan Highlands (subspecies *keniensis*), (2) Albertine Rift (*ruwenzori*), (3) northern Eastern Arc (*helleri*), and (4) south-central Eastern Arc, Ufipa and the Malawi Rift (*orientalis*). The estimated divergence times cluster remarkably around one of the three estimated peaks of aridification in Africa during the Plio-Pleistocene centred on 1 Myrs BP. Further, time to most recent common ancestor (TMRCA) estimates (1.7–1.6 Myrs BP) of gene divergence between the Albertine Rift and the other montane highlands corresponds closely with a second estimated peak of aridification at about 1.7 Myrs BP. Collectively, these results suggest that aridification of Africa in response to glaciation at higher latitudes during the Pleistocene has had a profound influence on montane speciation in east and central Africa.

Keywords: Glacial cycles; NCA; Gene flow; MIGRATE; MDIV; TMRCA; Coalescent; *Pogonocichla*

1. Introduction

The high amplitude glacial cycling of the upper Pleistocene and its consequent influence on vertebrate speciation (e.g., Pleistocene Refugia Model, Haffer, 1997; Mayr and O'Hara, 1986) has over the last decade received

* Corresponding author. Fax: +27 21 808 2405.
E-mail address: bowie@sun.ac.za (R.C.K. Bowie).

1055-7903/$ - see front matter © 2005 Elsevier Inc. All rights reserved.
doi:10.1016/j.ympev.2005.06.001

much criticism with molecular clock estimates suggesting that many (if not most) speciation events predate the large amplitude glacial cycles of the Pleistocene epoch (~2 Myrs BP) (Bowie et al., 2004a; García-Moreno and Fjeldså, 2000; Klicka and Zink, 1997; Roy et al., 1998, 2000; Zink and Slowinski, 1995). This is not to say that the high amplitude glacial cycling of the upper Pleistocene has not played an important role in shaping genetic structure and diversity in vertebrate populations (see Avise and Walker, 1998; Avise et al., 1998; Johnson and Cicero, 2004), only that these climatic perturbations may have had less of an influence on vertebrate speciation than previously thought.

Much emphasis has been placed on the evolution of Northern Hemisphere faunas in response to glacial cycles (e.g., Branco et al., 2002; Hewitt, 1996, 2000; Klicka and Zink, 1997, 2000; Knowles, 2001; Pfenninger and Posada, 2002; Taberlet et al., 1998). Few studies though have attempted to link the high-latitude climatic perturbations of the Pleistocene with the diversification of phylogenetic lineages of closely related species (e.g., Bowie et al., 2004a; Roy et al., 1998; Voelker, 1999) or within species in Africa (e.g., Bowie et al., 2004b), or other lower-latitude biomes (e.g., for Amazonia, Lessa et al., 2003).

The highly disjunct present-day distribution of African montane rainforest fauna and flora presents a biogeographical puzzle. Despite the often huge distances and unfavourable habitat between montane isolates, a large proportion of montane species reappear in even the most isolated forests (butterflies: Carcasson, 1964; birds: Diamond and Hamilton, 1980; Moreau, 1966; Prigogine, 1987; mammals: Kingdon, 1989, 1997; spiders: Griswold, 1991; and flora: Dowsett-Lemaire and Dowsett, 2001; White, 1983). Prigogine (1987) proposed a climatic-cycling model of repeated expansion and contraction events between forest blocks to explain this pattern; during wetter periods (inter-glacial at high latitudes) montane forest expanded to cover low-lying ridges and contracted again as Africa aridified in response to glaciation at high latitudes. From deep-sea cores, periods of aridity are estimated to have peaked near 2.8, 1.7, and 1.0 Myrs BP as the periodicity of glacial cycles altered (deMenocal, 1995, 2004). These changes in African climate are coincident with a shift to more arid and open vegetation conditions due to forest contraction, that in turn have been linked to major steps in the evolution of African hominids (deMenocal, 1995; Partridge et al., 1995; Templeton, 2002; Vrba, 1999) and bovids (Vrba, 1985).

If aridification of the Africa continent favoured arid-adapted species, montane forest species must have been disadvantaged as suitable habitat was reduced, and distributions became fragmented. Coupled to this, African montane forest birds are typically either: (1) sedentary, rarely dispersing more than a few kilometres from their natal sites; or (2) exhibit altitudinal movements in the cold non-breeding season, returning to montane forest to breed (Dowsett, 1982, 1985; Dowsett and Dowsett-Lemaire, 1984; Dowsett-Lemaire, 1988, 1989; Moreau, 1966) and are thus likely to show strong phylogeographical structure.

The a priori expectation of strong phylogeographical structure among African montane forest birds has been documented in studies of greenbuls (Roy et al., 1998) and sunbirds (Bowie et al., 2004a), although vicariance events were estimated to well predate the Pleistocene. Since climatic perturbations in Africa during the Pliocene (pre 2.5 Myrs BP) are poorly understood, these studies were unable to provide a link between glaciation-induced aridification of Africa and montane bird speciation. In an attempt to directly evaluate the relationship between aridification and montane bird population differentiation, we focus on the widely distributed Starred Robin (*Pogonocichla stellata*, Muscicapoidea) which, with its many subspecies (Fig. 1; Moreau, 1951; Oatley and Arnott, 1998), plumage and vocal polymorphisms (Moreau, 1951; Oatley and Arnott, 1998), provides a model organism to investigate the influence of global climatic perturbations on the genetic structure and diversity of an African montane bird. Specifically, we investigate the phylogeographical structure, genetic variability, and extent of gene flow within and among populations of Starred Robins across five broad geographical regions that encompass the spatially complex montane circle of Africa: (A) Kenyan Highlands, (B) Albertine Rift, (C) northern Eastern Arc, (D) central and southern Eastern Arc, and (E) the Ufipa Plateau and Malawi Rift (Fig. 1).

Given the extent of morphological and vocal diversity among Starred Robin populations around the montane circle of Africa (Moreau, 1951; Oatley and Arnott, 1998), we hypothesise that: (1) arid peaks around 1.7 and 1.0 Myrs BP that initiated a period of large-scale changes in the amplitude of climatic cycles (deMenocal, 1995) had a profound influence on the spatial structure of Starred Robin populations, with vicariant breaks between the five broad biogeographical regions being closely linked to these periods of increased aridity, and (2) that gene flow between some regions is now occurring as a consequence of the onset of more mesic conditions (inter-glacial) facilitating population expansion and dispersal and thus possible secondary contact among previously isolated lineages (e.g., Bowie et al., 2004b).

1.1. The Starred Robin

The Starred Robin (*Pogonocichla stellata*) is a small, brightly coloured forest robin, that typically breeds in montane forest between 1500 and 2200 m, and occasionally as high as 3300 m (Oatley and Arnott, 1998). In the adult male and female, the head and throat are deep grey-

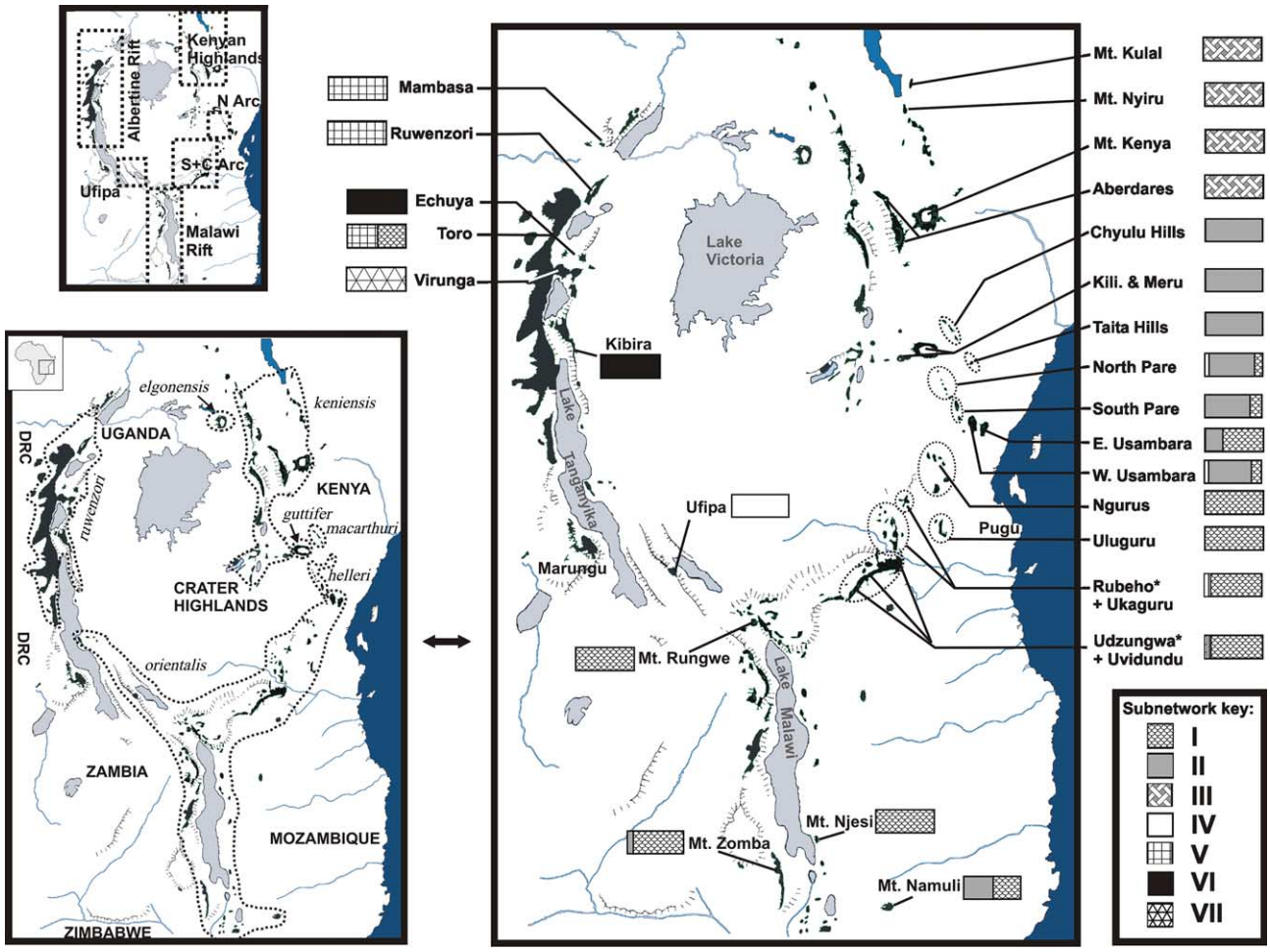

Fig. 1. Geographical distribution of the Starred Robin in east and central Africa, as well as the populations and taxa sampled from within the montane circle of Africa. Bar charts represent the frequency with which haplotypes from each of the seven subnetworks in Figs. 2 and 3 are present in each region. Populations denoted with an asterisk indicate that a number of haplotypes from other subnetworks are present in low frequency (see Appendix A for detail).

blue, the upperparts olive, underparts bright yellow, and the tail patterned black and yellow. The species is named after the white 'stars' on the head (supraloral spots) and lower throat. The species is distributed in montane forest extending from the Imatong Mountains in southern Sudan and Mt. Kulal (ca. 4°N) in Kenya, southwards across the eastern and central parts of the continent (Fig. 1). In South Africa, where latitude compensates for altitude, the Starred Robin reaches sea level at ca. 34°S. Only birds in adult plumage are known to breed, thus age at first breeding is not less than 2 years and more usually thought to be 3 years (Oatley and Arnott, 1998). In this study a generation time of 2.5 years was assumed.

The Starred Robin in the southern parts of its distribution is an altitudinal migrant, with females leaving breeding territories in winter and males tending to remain resident year round (Dowsett, 1982; Irwin, 1971; Moreau, 1951; Oatley, 1982; Oatley and Arnott, 1998). Although Dowsett (1982) suggests that some juvenile Starred Robins return to their natal sites, Oatley (1982), in an intensive mark-recapture study of Starred Robin populations in KwaZulu-Natal, South Africa, established that juveniles or subadults locally dispersed away from their birthplace and seldom returned. Immigrants from other populations move into forests at the onset of the subsequent breeding season and recruit into any vacant territories in the local population (Oatley, 1982). One important difference between the interpretations on Starred Robin philopatry is spatial scale. Dowsett (1982) was, in general, referring to philopatry in the context of juvenile birds recruiting into populations within the same geographical region (Nyika Plateau, Malawi). In contrast, Oatley (1982) was referring to recruitment into a specific forest population.

2. Methods

Mitochondrial DNA nucleotide sequences for the NADH 3 gene were collected from 283 individual birds.

To separate historical processes (e.g., vicariance) from recurrent processes (e.g., gene flow), a hierarchical analytical structure was followed. First a phylogeny of the identified haplotypes was constructed. This was followed by nested clade analysis (NCA; Templeton et al., 1987, 1992) of the associated statistical parsimony network to infer population history. NCA is considered an objective statistical method that attempts to reject a null hypothesis of no association between haplotype variation and geography, and then interprets significant patterns using an explicit set of criteria. Temporal information contained in the haplotype tree is used to partition current processes from historical processes to explain observed patterns of genetic variation. However, Knowles and Maddison (2002), in a recent simulation study suggested that NCA does not always infer the correct demographic and evolutionary processes that have led to the observed spatial distribution of haplotypes (but see Templeton, 2004). To test the validity of evolutionary patterns inferred from the NCA, coalescent modelling of directional gene flow (Beerli and Felsenstein, 1999, 2001) was also conducted. Independent analyses that assess concordance of hypothesised processes should provide a powerful framework for inferring patterns of diversification. Finally, to help separate secondary contact/current gene flow from the confounding effects of ancestral polymorphism (see Nielson and Wakeley, 2001) and, to estimate the time of gene divergence versus population divergence (see Edwards and Beerli, 2000), four parameters were simultaneously estimated using the Bayesian coalescent sampling method of Nielson and Wakeley (2001): population size (θ), time to most recent common ancestor (TMRCA), population divergence time, and the extent of gene flow among pairs of populations.

2.1. Population sampling

Tissue or blood samples were collected from 283 individuals from 58 sites representing 30 populations distributed around the montane circle of Africa (Appendix A, Fig. 1). In some cases, sites in the same mountain range were pooled and assumed to be from the same population (e.g., Mafwemiro and Uqwiva Forests in the Rubeho Mts). Of the seven northern montane subspecies recognised by Moreau (1951), six were sampled in this study: *keniensis* (= *intensa* + *pallidiflava*), *ruwenzori*, *guttifer*, *macarthuri*, *helleri*, and *orientalis*. No samples of *elgonensis* from Mt. Elgon were available. Unique DNA sequences have been submitted to GenBank under Accession Nos.: DQ074148–074205.

2.2. Laboratory procedures

DNA was extracted, PCR amplified for the NADH Dehydrogenase subunit 3 gene with flanking tRNAs and cycle sequenced as described in Bowie et al. (2004a). Sequences were obtained from both strands of DNA for each identified haplotype, as well as from an additional 65 individuals (total 123 individuals) to double-check that nucleotide bases were consistently called in single-stranded sequences. For the remaining individuals, only the forward strand was sequenced. All sequences were checked using the program Sequencher 3.0 (Gene Codes) and aligned to the chicken (*Gallus gallus*) mtDNA sequence (Desjardins and Morais, 1990) to test for the presence of any insertions, deletions or stop codons.

2.3. Phylogenetic analyses

Due to the large number of closely related haplotypes it was deemed more important to resolve affinities among the deeper branches of the tree than at the tips. Consequently, parsimony (MP) analyses were conducted using the Ratchet (Nixon, 1999), which is reported to be highly efficient at exploring tree space and therefore, finding alternative topologies. Search options for the MP ratchet were: 10% of the characters removed during each of 10,000 random addition replicates, five trees held for each iteration, and full tree-bisection-reconstruction (TBR) branch-swapping was implemented. The MP ratchet was conducted using NONA (Goloboff, 1999) running under the WINCLADA interface (Nixon, 1999). Clade support for the MP analysis was estimated using 1000 nonparametric bootstrap replicates (Felsenstein, 1985).

MrBayes 3.0 (Huelsenbeck and Ronquist, 2001) was used to conduct a Bayesian approach to phylogenetic inference. Four Metropolis-coupled MCMC chains (one cold and three heated chains) were run simultaneously to optimise efforts to find peaks in tree-space. The General Time Reversible model of nucleotide substitution with a gamma distribution (estimated using four rate categories) and invariable sites (GTR + I + G) was used in the Bayesian analyses. A Dirichlet distribution was assumed for estimation of the base frequency parameters and an uninformative (flat) prior was used for the topology. Trees were sampled every 500 generations in each of the three runs. This resulted in a sample of 20,001 trees (10 million generations), 10,001 trees (5 million generations), and 2001 trees (1 million generations), respectively. For each run, the first 25% of sampled trees were discarded. In both MP and BI analyses trees were rooted with *Sheppardia sharpei* and *Stiphrornis erythrothorax*, two other related members of the African Robin assemblage (Irwin and Clancey, 1974; Voelker and Bowie, unpublished data).

Due to the problems associated with the construction of intraspecific phylogenies (see Posada and Crandall, 2001), a statistical parsimony network among the 58 haplotypes was constructed using the program TCS ver. 1.01 (Clement et al., 2000).

2.4. Nested clade analyses (NCA)

The Templeton, Crandall, and Sing parsimony algorithm (Templeton et al., 1992) was used as an objective statistical approach to infer the population history of *Pogonocichla*. This is achieved by overlaying the evolutionary relationships among the haplotypes (phylogenetic tree/network) upon a spatial landscape (geography) of the geographical distributions of haplotypes and clades, thus integrating both time and space into a single analysis (Templeton, 2002). The TCS-derived statistical parsimony network was manually converted into a series of hierarchically nested clades using the rules in Templeton et al. (1987) and Templeton and Sing (1993). Calculation of NCA clade distances and permutation testing was conducted using the program GEODIS 2.0 (Posada et al., 2000). Statistical measures of significance were determined using the permutation procedure of Roff and Bentzen (1989) with 10,000 replicates. The most recent version of the inference key (Templeton, 2004; also posted online as 14 July 2004) was used to interpret results.

2.5. Coalescent-based estimates of gene flow and population divergence times

Although NCA provides a powerful analytical tool to infer population history, it does not allow for the estimation of parameters of interest such as gene flow among populations. Recent advances, based on the coalescent approach have made it possible to obtain directional maximum likelihood estimates of gene flow among populations while taking into account population structure and demographic processes (Beerli and Felsenstein, 1999, 2001). These analytical methods overcome the limitations imposed by traditional population genetic models, which usually rely on the biologically unrealistic assumptions of equal population sizes and symmetrical rate of gene flow among populations. Thus, the coalescent-based methods probably provide more robust estimates of gene flow than traditional F_{ST} based methods (Beerli and Felsenstein, 1999; Bossart and Prowell, 1998; Nielson and Wakeley, 2001).

There are inherent difficulties in unravelling the evolutionary history of a species, such as the Starred Robin, that has extensive genetic structure among a series of allopatric populations. Therefore, coalescent-based estimates of gene flow were used to: (1) seek support of inferences made using NCA and (2) determine estimates of gene flow between populations. Ideally, one should estimate all relevant parameters for the migration model, along with their likelihoods, but this is currently infeasible computationally. Pooling individuals into larger regional populations based on geography is a reasonable solution to circumvent computational difficulties, as well as to help resolve problems with estimating migration rates from small sample sizes (Pfenninger and Posada, 2002). Populations were pooled into five 'regional' populations, representing a priori defined montane areas of endemism (Bowie, 2003) as follows: (A) Kenyan Highlands (populations 7–11, Appendix A), (B) Albertine Rift (populations 1–6), (C) Northern Eastern Arc (populations 12–17), (D) Southern and Central Eastern Arc (populations 18–25), and (E) the Ufipa Plateau and Malawi Rift (populations 26–30).

Even for five populations, when long Markov-Chain-Monte-Carlo (MCMC, for explanation of this methodology, see Lewis, 2001) runs are implemented, computational time can be considerable (weeks). To make effective use of access to two 20-processor computer clusters available for these analyses, we decided to split the estimation procedure into several steps. First, a fully constrained migration parameter model was estimated, where only neighbouring populations exchanged migrants. Second, the five regional populations were divided into all possible combinations of groups of three populations and a fully resolved migration model was estimated for each of these triplets. Third, the information on relative migration rates from these triplet models was synthesised. Where there was consensus that no gene flow was taking place among triplets with pairs of populations in common, parameters between these population pairs were set to zero in a migration matrix. This matrix with user-defined zero migration between some population pairs (the partial constraints model) was subsequently used to estimate all remaining parameters among the five regional populations simultaneously. By eliminating parameters from the model, the statistical power with which the remaining parameters are estimated is increased. Peter Beerli provided a parallel version of MIGRATE, which, together with the standard Unix version (Beerli and Felsenstein, 1999, 2001), was used to estimate the above model on the 20-processor clusters.

For each migration analysis (the full constraints model, population triplets, and the partial constraints model), two analytical runs were conducted, an initial short run, followed by a second longer run. For both runs, the starting values of the population mutation parameter and the ratio between the immigration rate and the respective population and mutation rate per generation were estimated from F_{ST} values (Beerli and Felsenstein, 1999). For the long run (short run values in parentheses) 10 short chains, each with a total of 100,000 (10,000) generations and a sampling increment of 1000 (500) generations, and three long chains each with a total of 1,000,000 (100,000) generations and a sampling increment of 10,000 (5000) generations were run twice. For both, the short and long runs, the first 10,000 genealogies were discarded (the burnin). An adaptive heating scheme with four chains and a swapping interval of one was used. For the other settings, default values were implemented.

Many conventional methods for estimating gene flow (e.g., F_{ST} based approaches) are problematic. They do not allow for the simultaneous estimation of gene flow and divergence times and thus cannot separate recurrent gene flow from ancestral polymorphism. MIGRATE (Beerli and Felsenstein, 1999, 2001) does not do this either. To overcome this problem, we analysed our mtDNA sequence data using the Bayesian sampling coalescent-based method of Nielson and Wakeley (2001), implemented in the program MDIV (Nielson, 2002). MDIV is able to simultaneously estimate a variety of parameters: theta ($\theta = 2N_{ef}\mu$), migration rate ($M = 2N_{ef}m$), time of population divergence ($T = t/N_{ef}$) and time to most recent common ancestor (TMRCA $= t\mu$) from the same dataset, where N_{ef} is the female-effective population size, t is the generation time, and μ is the per locus mutation rate.

We used MDIV to estimate values of θ, M, T, and TMRCA for pairwise comparisons of each of the five biogeographical regions used in the MIGRATE analyses. Each pairwise simulation was repeated three times, one run of 2×10^6 generations and two runs of 5×10^6 generations with a 10% burnin. Multiple runs were conducted to determine if convergence in the mode of the posterior distribution was being reached. A finite-sites model with upper bounds of 10 migrants per generation and time of population divergence of 10 units was set as suggested by Nielson (2002). Values for θ, M, and T were plotted and the mode of the posterior distribution was accepted as the best estimate. Where possible, 95% credibility intervals were also estimated for each parameter. Standardised estimates for T and TMRCA are provided in which each estimate is multiplied by θ for the respective pairwise comparison to account for different effective population sizes and allow for direct comparison among estimates (Griswold and Baker, 2002). These values were converted into years before present using the widely assumed mutation rate of 2% per million years, or 1.915×10^{-5} substitutions per site per year, and a generation time of 2.5 years (for other recent examples using this methodology see Bulgin et al., 2003; Griswold and Baker, 2002).

3. Results

3.1. Genetic diversity

A 395 bp fragment of the mtDNA coding ND3 gene with flanking tRNA sequences was amplified (Chicken mtDNA 10,755–11,150; Desjardins and Morais, 1990) from 283 individuals representing six subspecies of the Starred Robin (*Pogonocichla stellata*). The aligned sequences were pruned at both the 5′ and the 3′ ends to remove missing data from the analysed dataset. This resulted in a final alignment of 383 bp per individual. A total of 58 unique haplotypes was found (Appendix A). The largest divergence was 6.3% (Kimura-2-parameter) between haplotypes 32 and 50 from Kahe Hill at the foot of Mt. Kilimanjaro (Tanzania) and Choha in the Ruwenzori Mts (Uganda).

Haplotype and nucleotide diversity were generally high within populations, with each biogeographical region having some populations with a comparatively high number of nucleotide differences from others within the same region. Within the Albertine Rift, Mambasa (population 1), the Ruwenzori Mts (population 2), and Echuya Forest (population 3), exhibited high nucleotide diversity despite relatively small samples sizes (Table 1). Nucleotide diversity in Toro (population 4) was more than 2.5 times greater than any other sampled population (Table 1). This was due to the presence of haplotypes characteristic of both the Albertine Rift and the South-central Eastern Arc being present at the same frequency (Appendix A, Fig. 1). Mt. Nyiru (population 8) and Mt. Kenya (population 10) had relatively high nucleotide diversity levels within the Kenyan Highlands. In contrast, 13 individuals from Mt. Kulal (population 7) all had the same unique haplotype. The Pare (populations 13 and 14) and Usambara Mts (populations 16 and 17) were genetically most diverse within the northern Eastern Arc, and within the southern and central Eastern Arc, the Udzungwa Highlands (population 15) harboured the greatest nucleotide diversity. Southern populations on Mt. Zomba (population 30) and Namuli (population 29) in the Malawi Rift and Mozambique Highlands, respectively, were as genetically diverse as populations from other regions around the montane circle. The Ufipa Plateau population (population 26) was genetically impoverished relative to the neighbouring Udzungwa Highlands.

3.2. Phylogenetic relationships among the haplotypes

Parsimony analyses (MP) of the 58 sampled haplotypes yielded 154 most parsimonious trees with a length of 294 steps (CI = 0.61, RI = 0.79, Fig. 2). Among the 383 bp analysed, 288 sites were constant, 41 (10.7%) sites were variable but parsimony uninformative and 54 (14.1%) sites were parsimony informative.

In the MP analyses, very few nodes had greater than 50% bootstrap support (Fig. 2). Similarly few nodes in the BI analysis had nodes with posterior probabilities of greater than 95% (Fig. 2). The marginal probabilities of the BI GTR + G + I model were estimated as follows: rate matrix, $r[G-T] = 1$, $r[C-T] = 38.34$, $r[C-G] = 0.89$, $r[A-T] = 0.97$, $r[A-G] = 58.3$, and $r[A-C] = 7.40$; base frequencies, A = 31%, C = 32%, G = 15%, and $T = 22\%$; α shape parameter G = 0.105 and the proportion of invariable sites I = 0.450.

Both analyses were concordant in identifying a few clusters of haplotypes that largely correlated with

Table 1
Genetic diversity indices for the 30 populations of Starred Robin sampled

No.		Haplotype diversity	Average number of differences	Nucleotide diversity ($\times 10^3$)
	Albertine Rift			
1	Mambasa ($n = 6$)	0.73 ± 0.15	1.9 ± 1.3	5.1 ± 3.8
2	Ruwenzori Mts ($n = 12$)	0.85 ± 0.10	2.7 ± 1.5	7.0 ± 4.5
3	Echuya Forest ($n = 3$)	1.0 ± 0.27	2.7 ± 1.9	7.0 ± 6.2
4	Toro ($n = 4$)	1.0 ± 0.18	7.3 ± 4.3	19.1 ± 13.6
5	Virunga Mts ($n = 2$)	1.0 ± 0.50	2.0 ± 1.7	5.2 ± 6.4
6	Kibira National Park ($n = 3$)	—	—	—
	Kenyan Highlands			
7	Mt. Kulal ($n = 13$)	—	—	—
8	Mt. Nyiru ($n = 4$)	0.50 ± 0.26	2.0 ± 1.4	5.2 ± 4.4
9	Aberdare Mts ($n = 24$)	0.63 ± 0.09	0.8 ± 0.6	2.2 ± 1.8
10	Mt. Kenya ($n = 4$)	0.83 ± 0.22	1.7 ± 1.2	4.3 ± 3.8
11	Chyulu Hills ($n = 4$)	—	—	—
	Northern Eastern Arc			
12	Taita Hills ($n = 10$)	0.67 ± 0.16	0.8 ± 0.6	2.1 ± 1.8
13	North Pare Mts ($n = 13$)	0.79 ± 0.11	2.6 ± 1.5	6.8 ± 4.4
14	South Pare Mts ($n = 5$)	0.70 ± 0.22	2.0 ± 1.3	5.2 ± 4.1
15	Kilimanjaro district ($n = 6$)	0.33 ± 0.21	1.3 ± 0.9	3.5 ± 2.9
16	West Usambara Mts ($n = 18$)	0.56 ± 0.13	1.8 ± 1.1	4.8 ± 3.2
17	East Usambara Mts ($n = 5$)	0.40 ± 0.24	1.6 ± 1.1	4.2 ± 3.4
	Southern and central Eastern Arc			
18	Nguru Mts ($n = 1$)	—	—	—
19	Ukaguru Mts ($n = 1$)	—	—	—
20	Pugu Hills ($n = 2$)	—	—	—
21	Rubeho Mts ($n = 39$)	0.51 ± 0.09	0.9 ± 0.7	2.5 ± 1.9
22	Morogoro ($n = 16$)	3.5 ± 0.15	0.4 ± 0.4	1.0 ± 1.1
23	Uvidundu Mts ($n = 3$)	0.67 ± 0.31	1.3 ± 1.1	3.5 ± 3.6
24	Uluguru Mts ($n = 17$)	0.59 ± 0.13	0.7 ± 0.5	1.8 ± 1.6
25	Udzungwa Highland ($n = 30$)	0.56 ± 0.11	1.6 ± 1.0	4.3 ± 2.9
	Ufipa Plateau and Malawi Rift			
26	Ufipa Plateau ($n = 16$)	0.32 ± 0.13	0.3 ± 0.3	0.8 ± 1.0
27	Mt. Rungwe ($n = 3$)	—	—	—
28	Mt. Njesi ($n = 1$)	—	—	—
29	Mt. Namuli ($n = 6$)	0.60 ± 0.13	2.4 ± 1.5	6.2 ± 4.5
30	Mt. Zomba ($n = 10$)	0.76 ± 0.13	1.5 ± 1.0	4.1 ± 3.0

traditional subspecific designations: (I) 18 haplotypes from the range of *orientalis* with a few individuals from the adjacent range of *helleri* in the Pare Mts (Tanzania, Fig. 2); (II) two groups of haplotypes, (a) haplotype 32 from Kahe, a hill with ground water forest situated between Mt. Kilimanjaro and the Pare Mts and (b) 13 haplotypes from SE Kenya and NE Tanzania that include *macarthuri* from the Chyulu Hills (Kenya, population 11), for which all four individuals sampled had the unique haplotype 25. Most of the remaining 12 haplotypes are found in the Taita Hills (Kenya), Pare Mts and Mt. Kilimanjaro. However, the most common haplotype sampled in this clade, hap. 2, is found disjunctly from NE Tanzania to Mt. Zomba (Malawi) and Mt. Namuli (Mozambique). Hap 35, which is closely allied with members of clade II, was sampled at Mt. Kilimanjaro and Mt. Meru (Tanzania). Thus, the range of *guttifer* may include Mt. Meru, but with only one sample from Mt. Meru, it is not reasonable to make definitive conclusions, especially considering that specimens from Mt. Meru are ascribed to *keniensis* based on morphology (Keith et al., 1992; Moreau, 1951). Excluding the Mt. Meru haplotype, the birds from the Kenyan Highlands (*keniensis*) form a monophyletic clade (clade III). Two haplotypes (hap. 4 and 45) were sampled from the 16 individuals from the Ufipa Plateau (clade IV). The most common of these, hap. 4, was found at low frequency in populations of both the central and northern parts of the Eastern Arc. Clades V–VII are collectively from the Albertine Rift, and constitute the northern half of the range of the subspecies *ruwenzori* (Fig. 1).

The largest average divergence value (4.33%) among the seven haplotype clusters (Fig. 2) was between Clade V (Ruwenzori Mts and SW Uganda) and the northeastern Arc (Clade II, Table 2). The lowest (0.77%) was between the Ufipa Plateau (Clade IV) and the geographically adjacent south-central Eastern Arc (Clade I). Divergence values within the Kenyan Highlands (Clade III, *keniensis*) are almost double that for any other

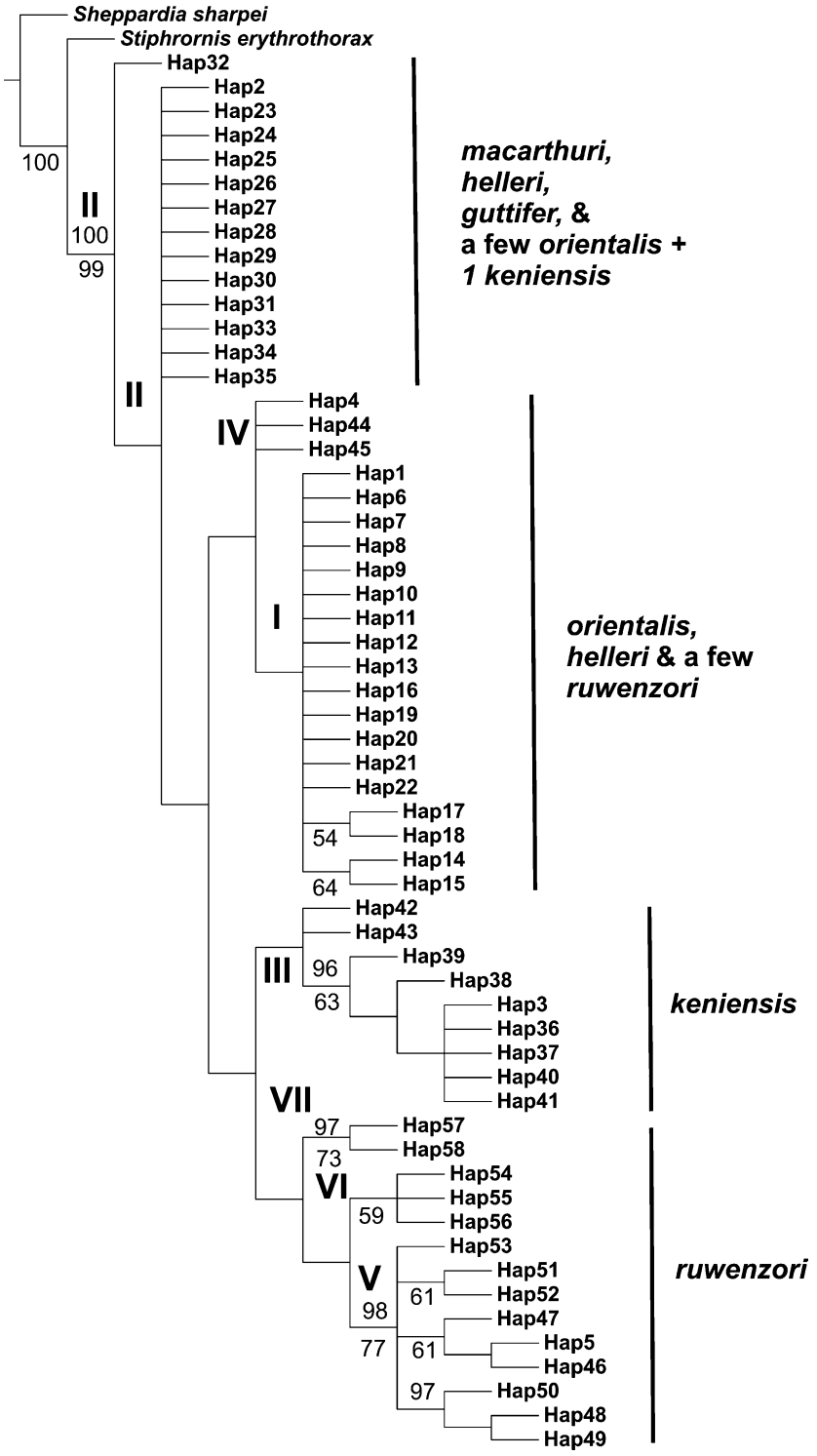

Fig. 2. Strict consensus of 154 equal length trees (L = 294, CI = 0.61, RI = 0.79) obtained using the parsimony ratchet. Seven clades of haplotypes were identified, which do not corroborate current subspecies boundaries (Fig. 1). Values below the nodes represent bootstrap support from 1000 replicates and values above the nodes BI posterior probability values from a 10 million generation run (burnin = 5000 trees, or 250,000 generations). Nodes are labelled only if supported by greater than 50% bootstrap support or a posterior probability greater than 95%.

regional population. This is largely due to Mt. Nyiru at the southern end of Lake Turkana having two divergent haplotypes (hap. 42 and 43). Divergence values between populations within the Albertine Rift (Clades V–VII, *ruwenzori*) are generally higher (2.41–3.54%) than between the Kenyan Highlands and the Eastern Arc (2.79–2.86%), or between the northern and southern Eastern Arc (1.85%).

Table 2
Average sequence divergence (Kimura-2-parameter) within (diagonal) and between haplotypes belonging to the seven subnetworks demarcated in Fig. 3 (mean below diagonal, standard deviation above diagonal)

	I	II	III	IV	V	VI	VII
South/Central Eastern Arc & Malawi Rift (I)	0.60 ± 0.18	0.36	0.54	0.19	0.38	0.58	0.33
Northern Eastern Arc (II)	1.85	0.87 ± 0.42	0.51	0.35	0.60	0.60	0.24
Kenyan Highlands (III)	2.79	2.86	1.56 ± 1.01	0.50	0.67	0.61	0.43
Ufipa Plateau (IV)	0.77	1.40	2.34	0.36 ± 0.16	0.30	0.55	0.20
Ruwenzori Mountains & Kabale (V)	3.57	4.33	3.92	3.08	0.95 + 0.38	0.56	0.31
Kibira National Park (VI)	3.67	3.69	3.6	3.16	3.19	0.75 ± 0.44	0.32
Virunga Highlands (VII)	3.15	3.22	2.96	2.74	3.54	2.41	0.55 ± 0.0

Subnetworks V–VII occur within the Albertine Rift.

3.3. Statistical parsimony network and nested design

Evaluation of the limits of statistical parsimony suggest that topologies connecting haplotypes by eight steps or fewer have a cumulative probability of greater than 95% being connected in a parsimonious fashion (i.e., without homoplasy). The inference of the haplotype network with the TCS program resulted in a network that can be broken into seven subnetworks (Fig. 3), which match those recovered in the phylogenetic analyses (Fig. 2). The seven subnetworks are: (I) the south-central Eastern Arc and Malawi Rift, (II) northern Eastern Arc, Chyulu Hills, Mt. Kilimanjaro and Mt. Meru, (III) Kenyan Highlands, (IV) Ufipa Plateau, (V) Ruwenzori Mts, northern Kabale and mountains to the southwest of Lake Edward, (VI) Kibira National Park, and (VII) the Virunga Highlands. Several mutational steps indicated by solid circles, representing either unsampled or extinct haplotypes separate the subnetworks from each other. Subnetworks I and II, are characterised by a star-like pattern, where the centrally located common 'ancestral' haplotype (Crandall and Templeton, 1993) is connected to several more recently derived haplotypes. Subnetwork V is ambiguously connected to subnetworks I, III, and VI (broken lines in Fig. 3) and an internal loop is suggested between haplotypes 47 and 49. These ambiguities result from the presence of more than one parsimonious connection between haplotypes.

In the final nested design, it makes little difference on how the loop within subnetwork V is resolved, as alternative nested designs do not change any of the inferred results in the NCA analyses. More difficult to resolve is how to link subnetwork V to the remaining network. The MP analysis (Fig. 2) suggests that all three subnetworks (V, VI, and VII) encompassing the Albertine Rift form a monophyletic clade, which is sister to the Kenyan Highlands (III). Thus, we connected subnetwork V to VI, Kibira National Park, because these sites fall within the same montane area of endemism and because of the hypothesised phylogenetic affinities. Strictly applying the nesting rules of Templeton et al. (1987) and Templeton and Sing (1993) results in the following higher level nesting structure [(3-1 + 3-2) (3-3 + 3-4)(3-5 + 3-6)], which form three 4-step clades in the final 5-step cladogram. This nesting structure, however, splits the Albertine Rift into two discreet groups, clade 3-4 (subnetwork VII from the Virunga Volcanoes) is united with the Kenyan Highlands, to the exclusion of the remaining Albertine Rift clades. This does not agree with the parsimony relationships among the different haplotypes (Fig. 2), where all haplotypes from the Albertine Rift form one monophyletic clade. As a result we repeated the NCA analyses using a simplified nesting structure [(3-1 + 3-2 + 3-3) (3-4 + 3-5 + 3-6)], which united the Kenyan Highlands with the Eastern Arc and Malawi Rift, but also united the three Albertine Rift subnetworks (V–VII) into a single 4-step clade. This is hereafter referred to as the preferred nesting structure (Fig. 3).

3.4. Nested clade analyses and inferred population history

The inferred population history underlying intraspecific genetic structure in the Starred Robin is dominated by the interaction of expansion events (dispersal–contiguous range expansion, isolation by distance) and contraction events (vicariance–fragmentation), which have occurred repeatedly, at multiple nested levels, during the Pleistocene (Figs. 4 and 5, Table 3).

Examining the significant geographically structured nesting levels suggests a number of processes occurring at different times throughout the Pleistocene. Genetic diversity in Starred Robin populations from the south-central Eastern Arc and Malawi Rift (subnetworks I and IV, clades, 2-1 and 1-1) appear to be driven by restricted gene flow with isolation by distance, or contiguous range expansion (Table 3). These evolutionary mechanisms are not opposed because both indicate an expansion of the ancestral range. Two fragmentation events were inferred. The more recent one (clade 1-7 in subnetwork II) separates the volcanic Chyulu Hills (hap. 25) from the rest of the northern Eastern Arc, and the older (clade 3-2) infers a fragmentation between the high volcanoes of Mt. Kilimanjaro and Meru from the older highlands of the Eastern Arc. At the 4-step clade level, two fragmentation events were also inferred: the

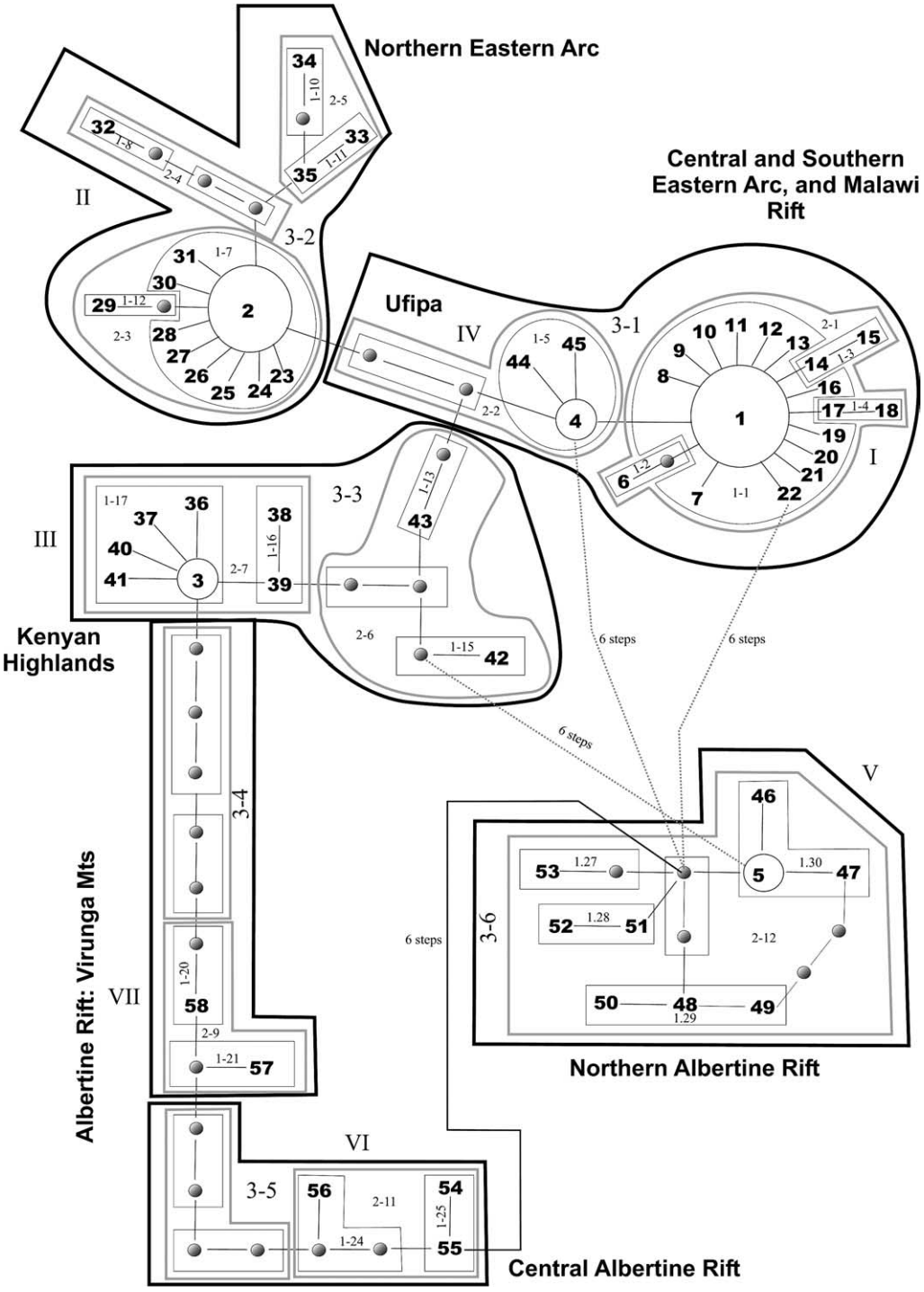

Fig. 3. Statistical parsimony network for the 58 Starred Robin haplotypes sampled with associated nested design; 1-step clades (narrow black lines), 2-step (broad grey lines), and 3-step clades (broad black lines). Each line in the network represents one mutational step. The five haplotypes with highest frequency are represented within circles, the area of which is proportional to the frequency with which the haplotype was sampled. Solid circles represent intermediate haplotypes that are necessary to link all observed haplotypes to the network. The intermediate haplotypes were either not sampled or have become extinct. Dotted lines point to ambiguities within the network, where there is more than one parsimonious way to make a connection. Seven subnetworks can be identified (I–VII), and are the same as those depicted in Fig. 2.

first leading to the separation of the Kenyan Highlands from the northern Eastern Arc and, the second splitting the Eastern Arc into a northern and south-central cluster of mountains (Fig. 5).

Within the Kenyan Highlands (subnetwork III, clade 3-3), a relatively deep intraspecific genetic divergence (1.5%) exists between haplotypes from Mt. Nyiru and the central Kenyan Highlands, Mt. Kenya, the

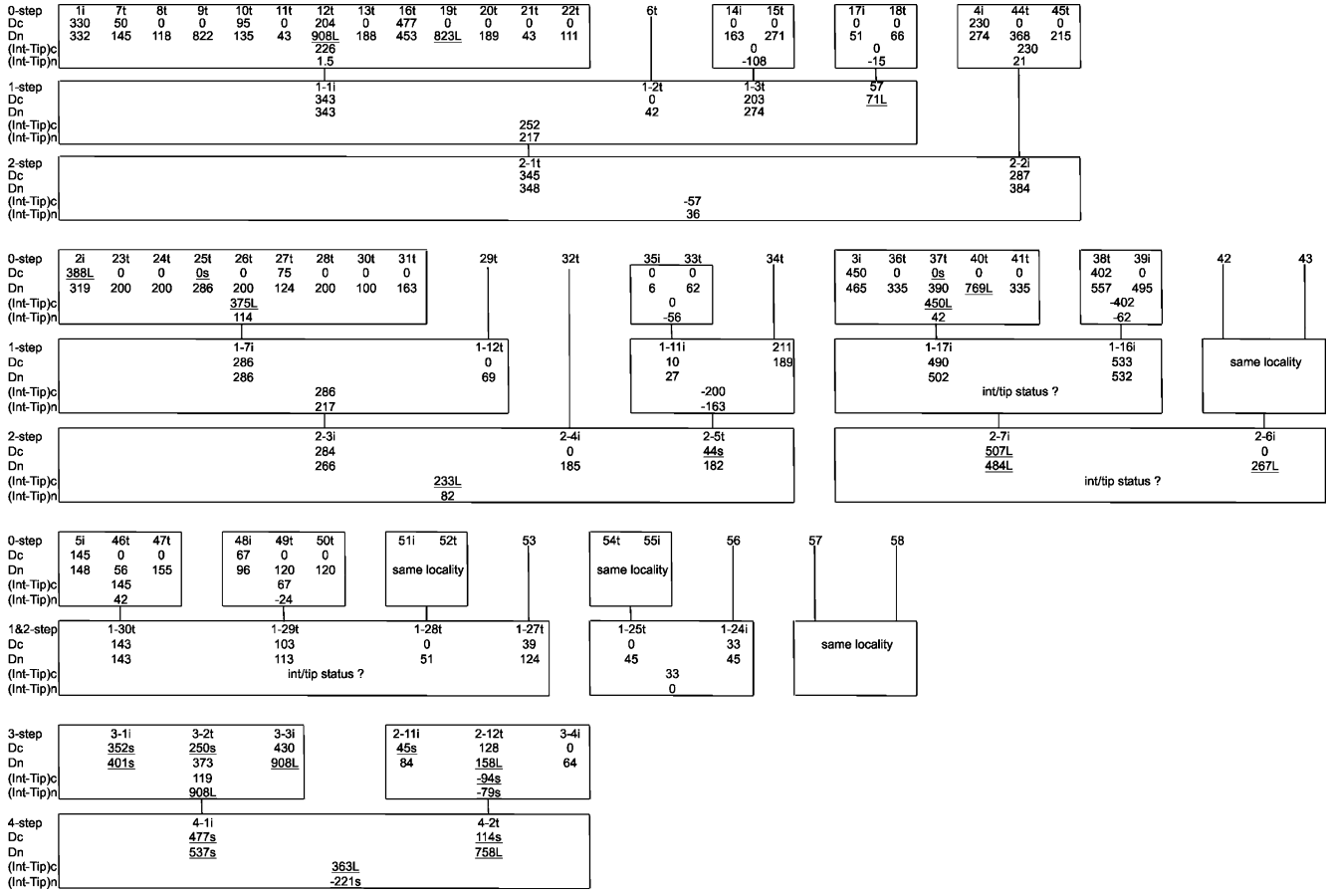

Fig. 4. Summary of the statistical results of the nested clade analysis of geographical distances for the 58 Starred Robin mtDNA haplotypes sampled. Haplotype numbers are the same as those in Appendix A and Figs. 2 and 3. The symbols, i or t designate a haplotype or clade as an interior or tip, respectively. Haplotypes nested in 1-step clades are grouped in boxes as represented in Fig. 3. Higher-level clades are designated as one moves down the figure. In each box, the clade distance (Dc) and nested clade distance (Dn) calculated for each clade within the nested group is shown, as well as the average difference in distances between interior and tip clades for Dc and Dn ([Int-Tip]c) and ([Int-tip]n), respectively. Significantly small or large distances (at $\alpha = 0.05$) are underlined and characterised by s or L, respectively.

Aberdares and hills in eastern Maralal. At lower levels (clade 1-17), restricted gene flow with some long distance dispersal is inferred between the central Kenyan Highlands, Mt. Kenya and Mt. Kulal.

Three subnetworks of haplotypes occur within the Albertine Rift (V, VI, and VII). Their evolutionary origins depend on how the higher level clades are nested. Under the preferred nesting structure with two 4-step clades [(3-1 + 3-2 + 3-3) (3-4 + 3-5 + 3-6)] an old contiguous range expansion is inferred within the Albertine Rift. If three 4-step clades are used [(3-1 + 3-2) (3-3 + 3-4) (3-5 + 3-6)] then haplotypes from the Virunga Volcanoes are nested with clade 3-3 from the Kenyan Highlands, suggesting that these areas may have been more recently connected.

The inference for the total cladogram (5-step clade) in either the preferred (clades 4-1 and 4-2) or alternative network (clades 4-1, 4-2, and 4-3) suggests that past fragmentation between the Albertine Rift, Kenyan Highlands, and Eastern Arc has historically shaped genetic variation among Starred Robin populations distributed around the montane circle of Africa (Table 3, Fig. 5).

3.5. Gene flow and the confouding influence of ancestral polymorphism

For the long and short runs (see Section 2), similar results were obtained, although the 95% confidence limits in the long run were smaller. In the full constraints model, where gene flow was limited to only neighbouring populations, no discernible gene flow was detected between the Kenyan Highlands (region A, Fig. 6) and Albertine Rift (region B, Fig. 6), or between the Kenyan Highlands and the northern Eastern Arc (region C) including surrounding volcanoes, Mt. Kilimanjaro, Mt. Meru, and the Chyulu Hills, supporting results of the NCA at the total cladogram (5-step clade) level. A negligible amount of gene flow ($4Nm < 1$) was inferred between the northern (region C), and the central and southern parts of the Eastern Arc (region D), with a slight asymmetry from south to

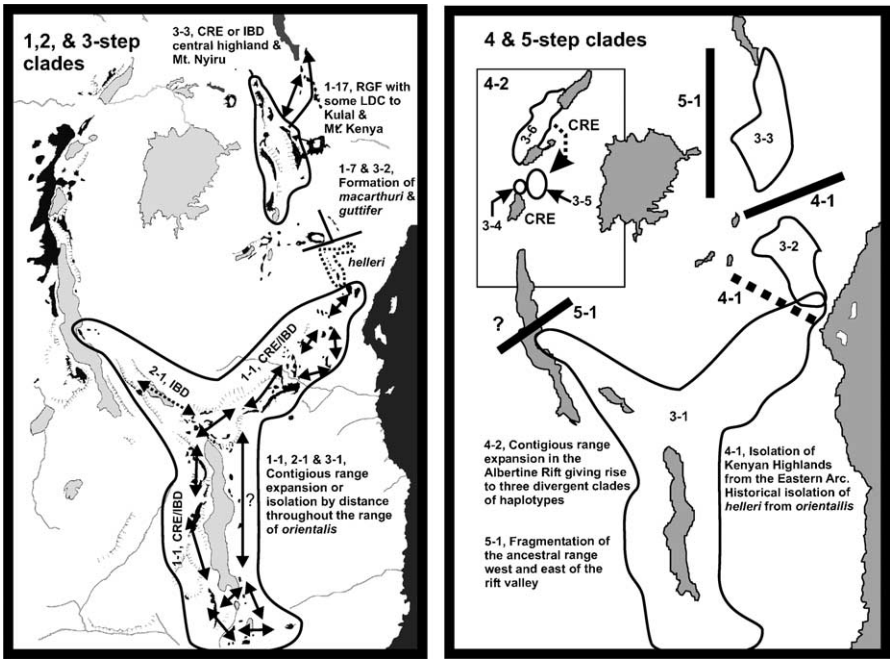

Fig. 5. Graphical summary of the major demographic events underpinning genetic diversity and structure in the Starred Robin that were identified using NCA (Fig. 4) and the preferred network structure (Fig. 3).

Table 3
Interpretation of the results of Fig. 4 using the most recent version of the inference key (Templeton, 2004, posted online as 14 July 2004)

Clade	Chain of inference	Demographic event inferred[a]
Preferred nested structure ((3.1 + 3.2 + 3.3) (3.4 + 3.5 + 3.6))		
1-1	1-2-11-17-NO	Inconclusive outcome (CRE or IbD)
1-7	1-2-3-4-9-NO	Past fragmentation
1-17	1-2-11-12-13-YES	LDC possibly coupled with subsequent fragmentation
2-1	1-2-11-17-4-NO	IbD
3-2	1-2-3-4-9-NO	Past fragmentation
3-3	1-2-?	Inconclusive outcome (CRE or IbD)
4-1	1-2-3-5-15-NO	Past fragmentation
4-2	1-2-11-12-NO	CRE
Total	1-2-3-5-15-NO	Past fragmentation
Alternative nested structure ((3.1 + 3.2) (3.3 + 3.4) (3.5 + 3.6))		
4-1	1-2-11-12-NO	CRE
4-2	1-2-?	Inconclusive outcome (CRE)
4-3	1-2-11-12-NO	CRE
Total	1-2-3-5-15-NO	Past fragmentation

Demographic inferences are presented both for the preferred nesting structure as well as the alternate nesting structure. One-step, 2-step, and 3-step clades remain the same for both nesting structures.

[a] *Abbreviations:* CRE, contiguous range expansion; IbD, restricted gene flow with isolation by distance; LDC, long distance colonisation.

north. Similarly, low values of gene flow ($4Nm = 1.3$) from the Albertine Rift (region B) to the Ufipa Plateau and Malawi Rift (region E) were detected but only in one direction. Considerable gene flow occurs between the central and southern Eastern Arc (region D), and the Ufipa Plateau and highlands of the Malawi Rift (region E), with a strong asymmetry from the Eastern Arc towards the more southerly populations (Fig. 6).

Three population sets, for all possible combinations among the five regions considered were used to develop a more complex, but realistic model of gene flow among Starred Robin populations. As in the full constraints model, results suggested that no, or negligible gene flow occurred between (1) the Kenyan Highlands (region A, Fig. 6) and the Albertine Rift (region B), (2) between the Kenyan Highlands and the southern and central Eastern Arc (region D), Ufipa Plateau and Malawi Rift (region E), or (3) between the Albertine and Malawi Rifts. In the partial constraints model the above migration parameters were set to zero (no gene flow), allowing the parameters to be estimated within the final model to be reduced from 25 to 17.

Coalescent analyses of the partial constraints model produced results among neighbouring populations as described above, but provided additional insights. (1) Gene flow is biased from the central and southern Eastern Arc (region D) towards the northern Eastern Arc (region C), with negligible gene flow in the opposite direction. (2) There is considerable genetic exchange between the northern Eastern Arc and surrounding volcanoes (region C) and, with the highlands of Malawi Rift (region E). A strong asymmetrical bias exists from north to south (Fig. 6). (3) A small amount of gene flow was inferred to occur between the Albertine Rift (region B) and the south-central Eastern (region D) Arc (Fig. 6).

The detection of gene flow, all be it small between the Albertine Rift (region B) and the south-central Eastern Arc (region D) is surprising, as it suggests that a bird which is known to only breed in montane forest, is

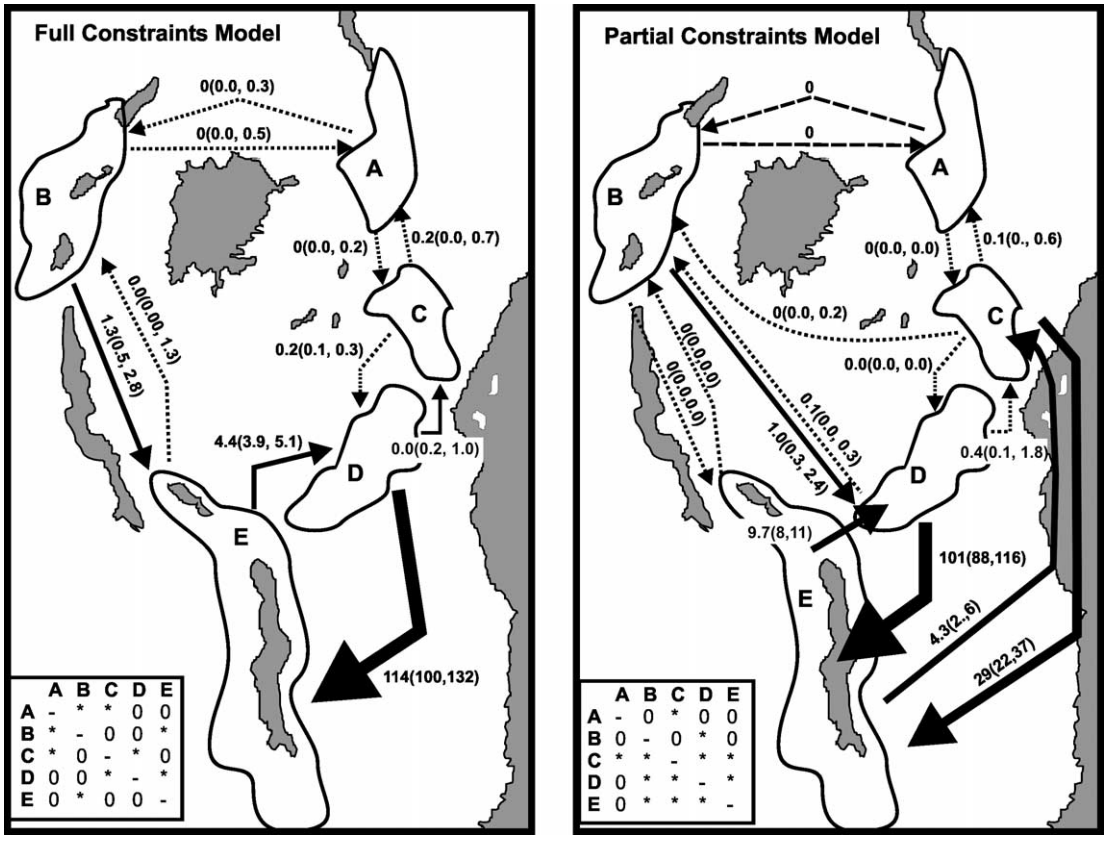

Fig. 6. Estimated migration parameters for the full constraint and partial constraint models of gene flow using MIGRATE. In the full constraint model of gene flow only neighbouring populations can exchange immigrants. The partial constraints model of gene flow was generated by first analysing all possible combinations of three-regional population triplets. Where gene flow was consistently negligible between two populations in all triplets bearing these populations, the parameters in the matrix were set to zero. This has the effect of reducing the number of parameters to estimate from 25 to 17, thereby increasing statistical power. Lines, which are dotted represent a migration rate of $4Nm < 0.5$. Solid lines are proportional to the extent to which immigration between two populations is taking place. Regional populations are: (A) Kenyan Highlands, (B) Albertine Rift, (C) Northern Eastern Arc, (D) Southern and central Eastern Arc and (E) Ufipa Plateau and the Malawi Rift.

actively dispersing across the savannah plains of the interior of Tanzania. This is in spite of the gene flow models suggesting that there is no dispersal between regions B and E, although there are highland forest patches along Lake Tanganyika (Figs. 1 and 6).

The coalescent simulation results obtained using MDIV exactly mirror the gene flow estimates obtained using the coalescent likelihood approach implemented in MIGRATE, with one important exception (Table 4). A negligible amount of gene flow ($4Nm = 0.34$ (0.08–0.96)) was estimated between the Albertine Rift (region B) and south-central Eastern Arc (region D). Coupled with one of the oldest estimates of population divergence at 1.2 Myrs BP, this result is consistent with a model of large divergence times with very small to no migration (=incomplete lineage sorting) rather than a model of short divergence times and low migration rates (recurrent gene flow). Therefore, it is doubtful that birds are dispersing across central Tanzania, and more likely that the haplotypes shared between the Albertine Rift (region B) and south-central Eastern Arc (region D) are a consequence of incomplete lineage sorting. Again these results corroborate the NCA results (Fig. 5, Table 3), which suggest these two populations were among the first to become isolated.

3.6. Estimates of gene versus population divergence times

Based on coalescent estimates of divergence times, gene divergence (when haplotypes first start to differentiate) took place between 1.6 and 1.0 Myrs BP. The Albertine Rift (region B, Fig. 6) appears to have been the first population to become isolated from the Eastern Arc (regions C and D), Ufipa and Malawi Rifts (region E) between 1.3 and 1.2 Myrs BP. The Albertine Rift appears to have maintained a connection with the Kenyan Highlands (region A) for a longer period of time, but became isolated from the Kenyan Highlands at around 0.9 Myrs BP, roughly the same time that the Kenyan Highlands became isolated from Eastern Arc between 0.9 and 0.8 Myrs BP. The northern (region C) and south-central Eastern Arc (region D) also diverged from each other at roughly the same time (0.8 Myrs BP) as the Kenyan Highlands became isolated from the Albertine Rift.

Given the inherent error associated with estimating divergence dates from molecular data, the estimates above should not be considered as absolute but rather as a rough guide to relative times of divergence among the five regions considered. Unfortunately, MDIV does not allow for confidence limits to be estimated around the TMRCA. The large disparity in estimates of TMRCA (gene divergence) versus population divergence (T) suggests that gene flow (Fig. 6, Table 4) has started to obscure the phylogeographical structure between populations in the Eastern Arc and Malawi Rifts.

4. Discussion

Genetic structure and diversity within populations of the Starred Robin distributed around the montane circle of Africa appears to have been initiated by at least two major vicariance events (5- and 4-step NCA clades in Fig. 5, Table 3), one that separated the Albertine Rift from all but the Kenyan Highlands 1.3–1.2 Myrs BP (Table 4), and another that separated the Kenyan Highlands from the northern Eastern Arc, and the northern Eastern Arc from the south-central Eastern Arc between 0.9 and 0.8 Myrs BP (Table 4). These values correspond with a lack of recurrent gene flow (Figs. 5 and 6, Table 4). The Albertine Rift and south-central Eastern Arc populations share haplotypes, but based on coalescent analyses, this can confidently be accounted for by ancestral polymorphism as opposed to recurrent gene flow (Table 4). Taken collectively, strong evidence exists for recognition of four major ancestral populations: (1) Kenyan Highlands (subspecies *keniensis*), (2) Albertine Rift (*ruwenzori*), (3) northern Eastern Arc (*helleri*) and (4) south-central Eastern Arc, Ufipa and the Malawi Rift (*orientalis*). Given the possibility of natal philopatry (Dowsett, 1982) and recognition of extensive plumage and vocal variation by the description of a relatively large number of subspecies (Moreau, 1951; Oatley and Arnott, 1998), this is perhaps not surprising and matches our a priori expectations.

The estimated population divergence (T) of the Albertine Rift from the Eastern Arc, Ufipa and Malawi Rifts dates to between 1.3 and 1.2 Myrs BP, and the subsequent isolation of the remaining populations (except regions D and E—south-central Eastern Arc, Ufipa and the Malawi Rift) to around 0.9–0.8 Myrs BP. These putative dates correspond remarkably with one of three estimated Plio-Pleistocene peaks of aridification in Africa (approx. 1 Myrs BP), which are thought to have occurred in response to a shift to larger amplitude glacial cycles interspersed with relatively short humid periods (deMenocal, 1995, 2004). Further TMRCA estimates (1.7–1.6 Myrs BP) of gene divergence between the Albertine Rift and the other montane highlands corresponds closely with a second estimated peak of aridification at about 1.7 Myrs BP (deMenocal, 1995). The high genetic diversity (Table 1) observed within the populations of each of the five major biogeographical regions also supports a long history of divergence among Starred Robin populations. Collectively, these results suggest that aridification of Africa in response to glaciation at high latitudes has had a profound influence on montane speciation in Africa.

Table 4
Pairwise estimates of θ (because the mutation rate is the same for each population, differences in θ correspond to differences in N_{ef} for each pair of populations), migration rates ($M = N_{ef}m$), time since divergence (T), and time to most recent common ancestor (TMRCA) based on analysis of mtDNA sequence data using MDIV

	Albertine Rift	Northern Eastern Arc	South-central Eastern Arc	Ufipa and Malawi Rifts
Kenyan Highlands	$\theta = 5.67$ [3.65–8.75]	$\theta = 4.55$ [2.84–6.85]	$\theta = 4.69$ [3.07–7.00]	$\theta = 2.00$ [1.13–3.84]
	$M = 0.06$ [0.00–0.46]	$M = 0.02$ [0.00–0.30]	$M = 0.02$ [0.00–0.44]	$M = 0.02$ [0.00–0.34]
(Region A)	$T = 0.9$ Myrs BP	$T = 0.9$ Myrs BP	$T = 0.8$ Myrs BP	$T = 0.7$ Myrs BP
	TMRCA = 1.6 Myrs BP	TMRCA = 1.3 Myrs BP	TMRCA = 1.5 Myrs BP	TMRCA = 1.0 Myrs BP
Albertine Rift		$\theta = 7.19$ [4.96–11.07]	$\theta = 6.68$ [4.67–9.89]	$\theta = 5.52$ [3.35–9.17]
		$M = 0.06$ [0.00–0.64	$M = 0.34$ [0.08–0.96]	$M = 0.26$ [0.04–1.54]
(Region B)		$T = 1.3$ Myrs BP	$T = 1.2$ Myrs BP	$T = 1.2$ Myrs BP
		TMRCA = 1.7 Myrs BP	TMRCA = 1.6 Myrs BP	TMRCA = 1.6 Myrs BP
Northern Eastern Arc			$\theta = 5.89$ [3.91–8.52]	$\theta = 4.10$ [2.27–6.42]
			$M = 1.14$ [0.44–2.60]	$M = 1.28$ [0.48 to >10]
Region (C)			$T = 0.8$ Myrs BP	$T = 0.3$ Myrs BP
			TMRCA = 1.5 Myrs BP	TMRCA = 0.9 Myrs BP
South-central Eastern Arc				$\theta = 4.12$ [2.63–6.52]
				$M = 8.34$ [1.19 to >10][a]
Region (D)				$T = 0.07$ Myrs BP
				TMRCA = 1.4 Myrs BP

The highest posterior probability scores for θ and M are given with their 95% credibility intervals. Estimates for T and $TRMCA$ are given in million years before present (Myrs BP) estimated according to Nielson and Wakeley (2001). A generation time of 2.5 years and a mutation rate of 1.915×10^{-5} substitutions per site per year was used to translate divergence times into Myrs BP. Regions correspond to those depicted in Fig. 6.

[a] Values are undefined for the upper credibility interval due to estimates for the parameter not converging on zero.

Despite obtaining 395 bp of mtDNA data, 58 haplotypes were recovered; what we consider to be enough variation for meaningful analyses using population genetic techniques. Though we think that somewhat longer sequences would have been better, we do not believe that this would have greatly altered the results of this study, other than possibly tightening some of the coalescent confidence intervals (see Edwards and Beerli, 2000). Although many studies have documented the effect of glaciation on the evolutionary history of Northern Hemisphere fauna (e.g., Branco et al., 2002; Griswold and Baker, 2002; Hewitt, 1996; Pfenninger and Posada, 2002), this study is the first to demonstrate how the indirect aridification of Africa caused by global cooling in response to glaciation at higher latitudes during the Plio-Pleistocene has influenced the evolutionary history of an African montane species.

4.1. Kenyan highlands

The central Kenyan Highlands form a large north–south extension on either side of the eastern Rift. Just to the east of the Aberdare Mts lies the relatively young volcano Mt. Kenya, and further north are a series of isolated massifs in semi-arid desert with montane forest restricted to their tops. The small northern outliers of the Kenyan Highlands, Mt. Kulal and Mt. Marsibit are not likely to have ever been directly connected with other mountains (Dowsett, 1985; Moreau, 1966). The low species diversity of their forest bird communities can be explained in terms of their small area and rare long-distance colonisation events. The NCA suggests that the evolution of both Starred Robin populations on Mt. Kenya and Mt. Kulal has arisen as a consequence of restricted gene flow with some long distance dispersal, a scenario that matches the a priori predictions given the spatial composition of the environment. The founding number on Mt. Kulal was most likely small, given that all 13 birds sampled had the same haplotype (hap. 37, Appendix A). The Starred Robin has never been recorded on Mt. Marsibit, a high massif, like Mt. Kulal, with a vanishing forest patch on its extreme upper margin in a matrix of semi-desert (Diamond and Keith, 1980; Friedmann and Stager, 1969; Lewis and Pomeroy, 1989; Moreau, 1951, 1966; L. Borghesio, in literature). This is despite apparently suitable habitat and the dispersal potential of the Starred Robin (Dowsett, 1982), emphasising the isolation of these mountains and the need for long-distance colonisation.

4.2. Albertine rift

Depending on how the higher-level clades are nested in the NCA analysis 1 to 2 contiguous range expansions are inferred, implying that more than one colonisation/isolation cycle may have occurred between the Albertine Rift and the Kenyan Highlands (Table 3). This is possible given that divergence estimates suggest that the Albertine Rift and Kenyan Highlands remained connected for another ~0.25 Myrs after the Albertine Rift became isolated from the other regions (Table 4). It is clear that the evolutionary history of Starred Robin populations within the Albertine Rift is complex. Indeed, one of the most unexpected findings of this study was the detection of three distinct subnetworks of haplotypes (Figs. 1–3) within the Albertine Rift, which apart from a brief note by Clancey (1972) has always been considered one taxon, *P. s. ruwenzori*. The spatial sampling currently is not detailed enough to accurately delimit subnetwork boundaries within the Albertine Rift, but additional genetic and morphological study is warranted.

4.3. Eastern Arc, Ufipa and Malawi rifts

Northeastern Tanzania and SE Kenya have a spatially complex distribution of Starred Robin subspecies in accordance with the juxtaposition of old and young mountains. *Pogonocichla s. helleri* is found in the Taita Hills and Pare Mts, that represent the most northerly mountain blocks of the Eastern Arc Mts (Fig. 1). Just to the northwest of the Taita Hills, *macarthuri* is restricted to the very young volcanic Chyulu Hills (ca. 40,000 yrs BP) and to the west *guttifer* is confined to the relatively young Mt. Kilimanjaro (ca. 1 Myrs BP; Griffiths, 1993) and possibly Mt. Meru (see Section 3). These populations, with the possible exception of *guttifer* (which differs from *keniensis* in only the saturation of colour) all have marked plumage differences (Dowsett, 1982; Moreau, 1951). In addition, *helleri* and *macarthuri* are reported to have a complex piping call, whereas *keniensis*, *guttifer*, *orientalis*, and *ruwenzori* have a more simple structure to their calls (Dowsett, 1982; Oatley and Arnott, 1998). The NCA analyses suggests that the isolation of *helleri* and *guttifer* (clades 4-1 and 3-2, respectively) is much more ancient than the isolation of *macarthuri* in the Chyulu Hills, in agreement with the young age of these volcanic mountains (see above). Both of the taxa from Mt. Kilimanjaro and the Chyulu Hills have unique haplotypes (Table 3).

Examination of gene flow (Fig. 6, Table 4) reveals that little to no gene flow exists within the Eastern Arc, with the wide gap of arid-lowland savannah separating the Nguru Mts (region D) from the northern Usambara and Pare Mts (region C). Coalescent modelling (Fig. 6, Table 4) also suggests that gene flow is taking place between the northern Eastern Arc (region C) and the more distant highlands of the Malawi Rift (region E), to the apparent exclusion of the more geographically proximate central and southern Eastern Arc (region D). This is unexpected, but it is possible that

dispersal between these areas could take place via coastal forests in Tanzania and Mozambique as the species has been observed as a seasonal (migrant) visitor in these forests (e.g., Pugu Hills, Table 1, Fig. 1; Burgess and Mlingwa, 2000).

4.4. Taxonomic considerations

Although there is considerable sequence diversity (ca. 6%), and strong phylogenetic structure among regions, it is apparent that some subspecies boundaries as currently defined from morphology, do not delineate evolutionarily significant entities. This is further complicated by inferences of gene flow among morphologically and vocally distinct forms. However, some regional populations of the Starred Robin (e.g., Kenyan Highlands—*keniensis* or Albertine Rift—*ruwenzori*) do appear to be both genetically and morphologically diagnosable, although not necessarily vocally distinct. Here, we refrain from detailed taxonomic revision because birds from the southern distribution of the Starred Robin's range were not sampled and other regional areas, for example the Albertine Rift, exhibited unexpected degrees of genetic structure in the apparent absence of morphological structure; a pattern, which given our limited sampling within the region is still incompletely understood.

Acknowledgments

We are grateful to the Tanzania Commission for Science and Technology, the Department of Ornithology at the National Museums of Kenya, the Kenyan Wildlife Service and governments of Uganda, Malawi, Mozambique and the Democratic Republic of the Congo for permission to collect and export specimens. We thank J. Kiure, D. Moyer, P. Ryan, D. Willard, B. Marks, T. Gnoske, J. Kerbis, S. Wamiti, B. Chege, P. Guichugi, and L. Borghesio for their help in collecting specimens. The Barrick Museum, University of Nevada is thanked for their loan of tissues from Mt. Zomba. For constructive comments on an earlier draft we thank T. Oatley, R. Zink, T. Smith, G. Voelker, and an anonymous reviewer. S. Ware helped with formatting. P. Beerli, R. Nielson, and C. Griswold are gratefully thanked for their help with the coalescent analyses. The Woods Hole and Cornell supercomputing centres are thanked for allowing us to make use of their computing facilities, without which the analyses reported in this study would have been very time consuming. The National Research Foundation (South Africa), the Danish Research Council, and the Skye Foundation and Charitable Trust, are thanked for providing funding for this project. The laboratory work for this project was carried out in the Field Museum's Pritzker Laboratory for Molecular Systematics and Evolution, operated with generous support of the Pritzker Foundation.

Appendix A

Populations, geographical coordinates, sample size, and haplotypes identified in each sampling locality

No.	Population	Country of origin	Geographical co-ordinates	*n*	Source[a]	Haplotypes[b]
	Albertine Rift					
1	Mambasa	Uganda	01.00N, 28.58E	6	FMNH	5(3) 47[1] 48(2)
2	Ruwenzori Mts	Uganda	00.25S, 30.00E	12	FMNH	5(5) 46[1] 48(1) 49(1) 50[1] 51[1] 52[1] 53(1)
3	Echuya Forest	Uganda	01.17S, 29.42E	3	FMNH	54[1] 55[1] 56(1)
4	Toro	Uganda	01.08S, 30.42E	4	ZMUC	1(1) 5(1) 12(1) 53(1)
5	Virunga Mts	Rwanda	01.40S, 29.60E	2	FITZ	57[1] 58[1]
6	Kibira National Park	Burundi	01.97S, 29.34E	3	FMNH	56(3)
	Kenyan Highlands					
7	Mt. Kulal	Kenya	02.72N, 36.93E	13	ZMUC	37(13)
8	Mt. Nyiru	Kenya	02.08N, 36.51E	4	ZMUC	43[3] 42[1]
9	Aberdare Mts	Kenya	00.06N, 36.67E	24	ZMUC	3(14) 36[2] 38(2) 39[5] 41[1]
10	Mt. Kenya	Kenya	00.17S, 37.02E	4	FITZ	3(1) 40[2] 38(1)
11	Chyulu Hills	Kenya	02.58S, 37.83E	4	FITZ	25[4]
	Northern Eastern Arc					
12	Taita Hills	Kenya	03.42S, 38.33E	10	LLENS	2(6) 23[1] 24[1] 26[1] 28[1]
13	North Pare Mts	Tanzania	03.72S, 37.58E	13	ZMUC	1(2) 2(6) 4(1) 27(1) 31[1] 33[1] 34(1)
14	South Pare Mts	Tanzania	04.26S, 37.83E	5	ZMUC	1(1) 2(3) 30[1]
15	Kilimanjaro	Tanzania	03.27S, 37.17E	6	ZMUC	32[1] 35(5)
16	West Usambara Mts	Tanzania	04.83S, 38.41E	18	ZMUC	1(2) 2(12) 4(1) 14[1] 27(1) 29[1]
17	East Usambara Mts	Tanzania	05.00S, 38.58E	5	ZMUC	1(4) 2(1)
	Southern and central Eastern Arc					
18	Nguru Mts	Tanzania	06.12S, 37.53E	1	ZMUC	1(1)

Appendix A (*continued*)

No.	Population	Country of origin	Geographical co-ordinates	*n*	Source[a]	Haplotypes[b]
19	Ukaguru Mts	Tanzania	06.35S, 36.88E	1	ZMUC	1(1)
20	Pugu Hills	Tanzania	06.88S, 39.08E	2	ZMUC	1(2)
21	Rubeho Mts	Tanzania	07.02S, 36.54E	39	ZMUC	1(27) 2(2) 4(3) 7(4) 8[1] 18[2]
22	Morogoro	Tanzania	07.10S, 36.64E	16	ZMUC	1(13) 7(1) 16(1) 22[1]
23	Uvidundu Mts	Tanzania	07.60S, 36.95E	3	ZMUC	1(2) 44[1]
24	Uluguru Mts	Tanzania	06.73S, 37.46E	17	ZMUC	1(11) 7(2) 10(1) 13[1] 16(1) 20[1]
25	Udzungwa Highland	Tanzania	07.96S, 36.06E	30	ZMUC	1(20) 5(1) 6[1] 10(1) 11(1) 12(1) 15[1] 17[2] 21[1] 34(1)
	Ufipa Plateau and Malawi Rift					
26	Ufipa Plateau	Tanzania	07.90S; 31.70E	16	ZMUC	4(13) 45[3]
27	Mt. Rungwe	Tanzania	09.20S, 33.60E	3	ZMUC	1(3)
28	Mt. Njesi	Mozambique	13.00S, 35.00E	1	FITZ	1(1)
29	Mt. Namuli	Mozambique	15.30S, 37.00E	6	FITZ	1(3) 2(3)
30	Mt. Zomba	Malawi	15.40S, 35.30E	10	FITZ/Barrick	1(5) 2(1) 9[1] 16(1) 19[2]

[a] Source codes: FMNH = Field Museum of Natural History, ZMUC = Zoological Museum of the University of Copenhagen, FITZ = Percy Fitz-Patrick Institute of African Ornithology, Barrick = The Barrick Museum, University of Nevada.

[b] Square brackets designate haplotypes unique to the specific population listed.

References

Avise, J.C., Walker, D., 1998. Pleistocene phylogeographic effects on avian populations and the speciation process. Proc. R. Soc. Lond. B 265, 457–463.

Avise, J.C., Walker, D., Jones, G.C., 1998. Speciation durations and Pleistocene effects on vertebrate phylogeography. Proc. R. Soc. Lond. B 265, 1707–1712.

Beerli, P., Felsenstein, J., 1999. Maximum likelihood estimation of a migration matrix and effective population sizes in two populations using a coalescent approach. Genetics 152, 763–773.

Beerli, P., Felsenstein, J., 2001. Maximum likelihood estimation of a migration matrix and effective population sizes in n subpopulations by using a coalescent approach. Proc. Natl. Acad. Sci. USA 98, 4563–4568.

Bossart, J.L., Prowell, D.P., 1998. Genetic estimates of population structure and gene flow: limitation, lessons, and new directions. Trends Ecol. Evol. 13, 202–206.

Bowie, R.C.K, 2003. Birds, molecules, and evolutionary patterns among Africa's Islands in the sky. Ph.D. thesis, University of Cape Town, South Africa.

Bowie, R.C.K., Fjeldså, J., Hackett, S.J., Crowe, T.M., 2004a. Systematics and biogeography of Double-collared sunbirds from the Eastern Arc Mountains, Tanzania. Auk 121, 660–681.

Bowie, R.C.K., Fjeldså, J., Hackett, S.J., Crowe, T.M., 2004b. Molecular evolution in space and through time: mtDNA phylogeography of the Olive Sunbird (*Nectarinia olivacea/obscura*) throughout continental Africa. Mol. Phylogenet. Evol. 33, 56–74.

Branco, M., Monnerot, M., Ferrand, N., Templeton, A.R., 2002. Postglacial dispersal of the European Rabbit (*Oryctolagus cuniculus*) on the Iberian Peninsula reconstructed from nested clade and mismatch analyses of mitochondrial DNA genetic variation. Evolution 56, 792–803.

Bulgin, N.L., Gibbs, H.L., Vickery, P., Baker, A.J., 2003. Ancestral polymorphism in genetic markers obscure detection of evolutionary distinct populations in the endangered Florida grasshopper sparrow (*Ammodramus savannarum floridanus*). Mol. Ecol. 12, 831–844.

Burgess, N.D., Mlingwa, C.O.F., 2000. Evidence for altitudinal migration of forest birds between montane Eastern Arc and lowland forests in East Africa. Ostrich 71, 180–190.

Carcasson, R.H., 1964. A preliminary survey of the zoogeography of African butterflies. E. Afr. Wildl. J. 2, 122–157.

Clancey, P.A., 1972. Miscellaneous taxonomic notes on African Birds No. 34. Durban Mus. Novitates 9, 145–162.

Clement, M., Posada, D., Crandall, K.A., 2000. TCS: a computer program to estimate gene genealogies. Mol. Ecol. 9, 1657–1660.

Crandall, K.A., Templeton, A.R., 1993. Empirical tests of some predictions from coalescent theory with application to intraspecific phylogeny reconstruction. Genetics 134, 959–969.

deMenocal, P.B., 1995. Plio-Pleistocene African climate. Science 270, 53–59.

deMenocal, P.B., 2004. African climate change and faunal evolution during the Pliocene–Pleistocene. Earth Planetary Sci. Lett. 220, 3–24.

Desjardins, P., Morais, R., 1990. Sequence and gene organisation of the chicken mitochondrial genome. A novel gene order in higher vertebrates. J. Mol. Evol. 212, 599–634.

Diamond, A.W., Hamilton, A.C., 1980. The distribution of forest passerine birds and Quaternary climatic change in Africa. J. Zool. (Lond.) 191, 379–402.

Diamond, A.W., Keith, G.S., 1980. Avifaunas of Kenya Forest islands. 1- Mt. Kulal. Scopus 4, 49–55.

Dowsett, R.J., 1982. The population dynamics and seasonal dispersal of the Starred Robin (*Pogonocichla stellata*). MSc Thesis, University of Natal, South Africa.

Dowsett, R.J., 1985. Site-fidelity and survival rates of some montane forest birds in Malawi, south-central Africa. Biotropica 17, 145–154.

Dowsett, R.J., Dowsett-Lemaire, F., 1984. Breeding and moult cycles of some montane forest birds in south-central Africa. Review Ecology (Terre et Vie) 39, 89–111.

Dowsett-Lemaire, F., 1988. On the breeding behaviour of three montane sunbirds *Nectarinia* spp. in northern Malawi. Scopus 11, 79–86.

Dowsett-Lemaire, F., 1989. Food plants and the annual cycle in a montane community of sunbirds (*Nectarinia* spp.) in northern Malawi. Tauraco 1, 167–185.

Dowsett-Lemaire, F., Dowsett, R.J., 2001. African forest birds: patterns of endemism and species richness. In: Weber, W. (Ed.), African Rain Forest Ecology and Conservation: An Interdisciplinary Perspective. Yale University Press, New Haven, pp. 233–262.

Edwards, S.V., Beerli, P., 2000. Gene divergence, population divergence, and the variance in coalescence time in phylogeographic studies. Evolution 54, 1839–1854.

Felsenstein, J., 1985. Confidence limits of phylogenies: an approach using the bootstrap. Evolution 39, 783–791.

Friedmann, H., Stager, K.E., 1969. Results of the 1964 Cheney Tanganyikan Expedition Ornithology. Contributions to Science Los Angeles Mus. 84: 1–1 50.

García-Moreno, J., Fjeldså, J., 2000. Chronology and mode of speciation in the Andean Avifauna. In: Rheinwald, G. (Ed.), Isolated Vertebrate Communities in the Tropics, Proceedings of the Fourth International Symposium, Bonn. Zool. Monogr. 46, pp. 25–46.

Goloboff, P., 1999. NONA ver. 2 Published by the author, Tucumán, Argentina.

Griffiths, C.J., 1993. The geological evolution of East Africa. In: Lovett, J.C., Wasser, S.K. (Eds.), Biogeography and Ecology of the Rain Forests of Eastern Africa. Cambridge University Press, Cambridge, UK, pp. 9–21.

Griswold, C.E., 1991. Cladistic biogeography of afromontane spiders. Aust. Syst. Biol. 4, 73–89.

Griswold, C.K., Baker, A.J., 2002. Time to most recent common ancestor and divergence times of populations of common Chaffinches (*Fringilla coelebs*) in Europe and North Africa: insights into Pleistocene refugia and current levels of migration. Evolution 56, 143–153.

Haffer, J., 1997. Alternative models of vertebrate speciation in Amazonia: an overview. Biodiv. Cons. 6, 451–476.

Hewitt, G.M., 1996. Some genetic consequences of ice ages, and their role in divergence and speciation. Biol. J. Linn. Soc. 58, 247–276.

Hewitt, G.M., 2000. The genetic legacy of the Quaternary ice-ages. Nature 405, 907–913.

Huelsenbeck, J.P., Ronquist, F., 2001. Mr Bayes: a program for the Bayesian inference of phylogeny.

Irwin, M.P.S., 1971. The Starred Bush Robin *Pogonocichla stellata* in eastern Rhodesia and adjacent Mozambique. Bull. B.O.C. 91, 14–18.

Irwin, M.P.S., Clancey, P.A., 1974. A re-appraisal of the generic relationships of some African forest-dwelling robins (Aves: Turdudae). Arnoldia (Rhodesia) 6, 1–19.

Johnson, N.K., Cicero, C., 2004. New mitochondrial DNA data affirm the importance of Pleistocene speciation in North American birds. Evolution 58, 1122–1130.

Keith, S., Urban, E.K., Fry, C.H., 1992. In: The Birds of Africa, vol. IV. Academic Press, London.

Kingdon, J., 1989. Island Africa. Princeton University Press, New Jersey.

Kingdon, J., 1997. The Kingdon Field Guide to African Mammals. Academic Press, New York.

Klicka, J., Zink, R.M., 1997. The importance of recent ice ages in speciation: a failed paradigm. Science 277, 1666–1669.

Klicka, J., Zink, R.M., 2000. Pleistocene effects on North American songbird evolution. Proc. R. Soc. Lond. B 166, 695–700.

Knowles, L.L., 2001. Did the Pleistocene glaciations promote divergence. Tests of explicit refugial models in montane grasshoppers. Mol. Ecol. 10, 691–701.

Knowles, L.L., Maddison, W.P., 2002. Statistical phylogeography. Mol. Ecol. 11, 2623–2635.

Lessa, E.P., Cook, J.A., Patton, J.L., 2003. Genetic footprints of demographic expansion in North America, but not Amazonia, during the late Quaternary. Proc. Natl. Acad. Sci. USA 100, 10331–10334.

Lewis, A., Pomeroy, D., 1989. A Bird Atlas of Kenya. A.A. Balkema, Rotterdam pp. 620.

Lewis, P.O., 2001. Phylogenetic systematics turns over a new leaf. Trends Ecol. Evol. 16, 30–37.

Mayr, E., O'Hara, R.J., 1986. The biogeographic evidence supporting the Pleistocene Forest Refuge Hypothesis. Evolution 40, 55–66.

Moreau, R.E., 1951. Geographical variation and plumage sequence in Pogonocichla. Ibis 93, 383–401.

Moreau, R.E., 1966. The Bird Faunas of Africa and its Islands. Academic Press, London.

Nielson, R., 2002. MDIV software. Available from: <http://www.biom.cornell.edu/Homepages/Rasmus_Nielson/files.html>.

Nielson, R., Wakeley, J., 2001. Distinguishing migration from isolation: a Markov Chain Monte Carlo approach. Genetics 158, 885–896.

Nixon, K.C., 1999. The parsimony ratchet, a new method for rapid parsimony analysis. Cladistics 15, 407–414.

Nixon, K.C., 1999-2002. WinClada ver. 1.0000 Published by the author, Ithaca, NY, USA.

Oatley, T.B., 1982. The Starred Robin in Natal, Part 2: Annual cycles and feeding ecology. Ostrich 53, 193–205.

Oatley, T.B., Arnott, G., 1998. Robins of Africa. Acorn Books, Randberg, South Africa.

Partridge, T.C., Wood, B.A., deMenocal, P.B., 1995. The influence of global climatic change and regional uplift in large-mammalian evolution in East and Southern Africa. In: Vrba, E.S., Denton, G.H., Partridge, T.C., Burckle, L.H. (Eds.), Paleoclimate and Evolution, with Emphasis on Human Origins. Yale University Press, New Haven, pp. 331–355.

Pfenninger, M., Posada, D., 2002. Phylogeographic history of the land snail *Candidula unifasciata* (Helicellinae, Stylommatophora): fragmentation, corridor migration and secondary contact. Evolution 56, 1776–1788.

Posada, D., Crandall, K.A., 2001. Intraspecific gene genealogies: tree grafting into cladograms. Trends Ecol. Evol. 16, 37–45.

Posada, D., Crandall, K.A., Templeton, A.R., 2000. GeoDis: a program for the cladistic nested analysis of the geographical distribution of genetic haplotypes. Mol. Ecol. 9, 487–488.

Prigogine, A., 1987. Disjunctions of montane birds in the Afrotropical region. Bonn. Zool. Beitr. 38, 195–207.

Roff, D.A., Bentzen, P., 1989. The statistical analysis of mitochondrial DNA polymorphisms: chi-squared and the problem of small sample sizes. Mol. Biol. Evol. 6, 539–545.

Roy, M.S., Arctander, P., Fjeldså, J., 1998. Speciation and taxonomy of montane greenbuls of the genus *Andropadus* (Aves: Pycnonotidae). Steenstrupia 24, 51–66.

Roy, M.S., Sponer, R., Fjeldså, J., 2000. Molecular systematics and evolutionary history of Akalats (Genus *Sheppardia*): a pre-Pleistocene radiation in a group of African forest birds. Mol. Phylogenet. Evol. 18, 74–83.

Taberlet, P., Fumagalli, L., Wust-Saucy, A.G., Cosson, J.F., 1998. Comparative phylogeography and postglacial colonisation routes in Europe. Mol. Ecol. 7, 453–464.

Templeton, A.R., 2002. Out of Africa again and again. Nature 416, 45–51.

Templeton, A.R., 2004. Statistical phylogeography: methods of evaluating and minimizing inference events. Mol. Ecol. 13, 789–809.

Templeton, A.R., Sing, C.F., 1993. A cladistic analysis of phenotypic associations with haplotypes inferred from restriction endonuclease mapping. IV. Nested analyses with cladogram uncertainty and recombination. Genetics 134, 659–669.

Templeton, A.R., Boerwinkle, E., Sing, C.F., 1987. A cladistic analysis of phenotypic associations with haplotypes inferred from restriction endonuclease mapping and DNA sequence data. I. Basic theory and an analysis of alcohol dehydrogenase activity in *Drosophila*. Genetics 117, 343–351.

Templeton, A.R., Crandall, K.A., Sing, C.F., 1992. A cladistic analysis of phenotypic associations with haplotypes inferred from restriction endonuclease mapping and DNA sequence data. III. Cladogram estimation. Genetics 132, 619–633.

Voelker, G., 1999. Dispersal, vicariance and clocks: historical biogeography and speciation in a cosmopolitan passerine genus (*Anthus*: Motacillidae). Evolution 53, 1536–1552.

Vrba, E.S., 1985. African Bovidae: evolutionary events since the Miocene. S. Afr. J. Sci. 81, 263–266.

Vrba, E.S., 1999. Habitat theory in relation to the evolution in African Neogene biota and Hominids. In: Bromage, T.G., Schrenk, S. (Eds.), African Biogeography, Climate Change and Human Evolution. Oxford University Press, Oxford, pp. 19–34.

White, F., 1983. The vegetation of Africa. UNESCO, Paris.

Zink, R.M., Slowinski, J.B., 1995. Evidence from molecular systematics for decreased avian diversification in the Pleistocene Epoch. Proc. Natl. Acad. Sci. USA 92, 5832–5835.